ELECTRONIC SUPPLEMENTARY INFORMATION

Physicochemical surface-structure studies of highly active zirconocene polymerisation catalysts on solid polymethylaluminoxane activating supports

Alexander F. R. Kilpatrick,† Nicholas H. Rees,† Zoë R. Turner,† Jean-Charles Buffet† and Dermot O'Hare†*

†Chemistry Research Laboratory, Department of Chemistry, University of Oxford, 12 Mansfield Road, Oxford, OX1 3TA, U.K.

Table of contents

1. Experimental details

1.1. General procedures

All manipulations were carried out using standard Schlenk techniques under N_2,[1] or in an MBraun UNIlab glovebox under N_2. All glassware was dried at 160 °C overnight prior to use. Sonications were carried out in a 9.2 L volume VWR ultrasonic bath (dry running frequency 45 kHz) with built-in digital timer and thermostat. Hexane and toluene were dried and degassed using an MBraun SPS-800 solvent purification system.[2] Dried solvents were collected, degassed and stored over N_2 in K mirrored ampules. THF–d_8 (Fluorochem) was degassed by three freeze−pump−thaw cycles, dried by refluxing over CaH_2 for three days, vacuum distilled into a J. Young ampoule and stored under N_2. Trimethylaluminium (TMA), tri*iso*butylaluminium (TIBA) and benzoic acid (BA, 99%) were supplied by Aldrich and used as received. Solid polymethylaluminoxane (sMAO, 40.2 $wt\%_{Al,}$)[3,4] and bis(cyclopentadienyl)zirconium(IV) dimethide were synthesised according to literature procedures. Bis(cyclopentadienyl)zirconium(IV) dichloride (Aldrich), bis-(*n*-butylcyclopenta-dienyl)-zirconium(IV) dichloride (MCAT), and *rac*-ethylenebis(indenyl)-zirconium(IV) dichloride (Strem) were used as received. Nitric acid (68% d=1.42, Primar Plus™, for trace metal analysis) was supplied by Fisher Scientific.

1.2. Analytical techniques

Solution NMR samples were prepared in the glovebox, using 5 mm J. Young tap NMR tubes. Spectra were measured either on a Bruker Avance III HD nanobay 400 MHz NMR spectrometer, or a Bruker Avance III 500 MHz NMR spectrometer and were referenced internally to the residual protic solvent (^{1}H) or the signals of the solvent (^{13}C), and aqueous $Al(NO_3)_3$ for ^{27}Al. Peak fittings and integrations of NMR spectra were carried out using the MestReNova software package.[5]

Oxford: Solid state NMR samples were packed in the glovebox, using powdered solid material loaded into 3.2 or 4.0 mm zirconia rotors. Spectra were measured on a Bruker Avance III HD 400 MHz NMR spectrometer at room temperature. ^{27}Al Hahnecho spectra of sMMAO samples employed a recycle delay of 0.01 s, 32000 scans and a spinning speed of 15 kHz. ^{1}H and ^{19}F DEPTH spectra used a recycle delay of 10 s, 32 scans and a spinning speed of 10 and 15 kHz. ^{13}C CPMAS spectra were acquired with cross polarisation from ^{1}H (contact time 4.0 ms, recycling delay 5 s, 5000 scans) and ^{19}F (contact time 0.9 ms, recycling delay 120 s, 480 scans) with either ^{1}H (for non fluorine containing samples) or dual ^{1}H/^{19}F decoupling. ^{29}Si CPMAS employed a contact time of 5.5 ms, a recycle delay of 10 s, and 240 scans. Spectral referencing is with respect to external, adamantane for ^{13}C (38.52 ppm) and ^{1}H (1.85 ppm), $CFCl_3$ for ^{19}F (0.00 ppm), aqueous $Al(NO_3)_3$ for ^{27}Al (0.00 ppm) and kaolinite for ^{29}Si (91.7 ppm).

Warwick: High field static NMR experiments were carried out at the UK 850 MHz solid-state NMR facility at the University of Warwick, with assistance from Dr D. Iuga (University of Warwick). Samples were prepared in a nitrogen flushbox, using powdered solid material loaded into 7 mm o.d. silicon nitride rotors (to avoid the background ^{91}Zr signal reported when using zirconia rotors).[6] Spectra were measured at room temperature on a Bruker WB US^2 850 MHz NMR spectrometer for which

$\nu_0(^{91}Zr)$ = 79.04 MHz. Spectra were acquired on a 7 mm low gamma H13895 single channel probe. The QCPMG pulse sequence was employed.[7] using $1/\tau_a$ = 1707.58 Hz, 40512 scans, sweep width 1.0 MHz. A total of five subspectra at offset frequencies −82011.77, −30591.77, 20828.23, 72248.23 and 123668.23 Hz were measured as part of the piece-wise acquisition. The spectra were analysed in Bruker TopSpin™ 3.2 software package, subjected to a magnitude correction and co-added to obtain the complete lineshape. Spectral referencing is with respect to a saturated CH_2Cl_2 solution of Cp_2ZrCl_2, δ_{iso} = 0.0 ppm.

Diffuse reflectance infrared Fourier transform (DRIFT) spectroscopy samples were prepared as powders in an alumina crucible and sealed under N_2 in a Pike Technologies gas-tight cell. Spectra were measured at room temperature through a NaCl window on a Bruker VERTEX 80 FT-IR spectrometer fitted with a Pike Technologies DiffusIR accessory, using 64 scans, resolution 4 and spectral range 4500–400 cm^{-1}. These spectra were collected in reflectance units and submitted to Kubelka–Munk transform.[10] A background spectrum (128 scans) of a pristine gold surface under N_2 was recorded before each set of measurements.

Samples for ICP-MS analysis were prepared by digestion in high purity HNO_3 solution (2 h reflux), and dilution with 18.2 Mohm DI water, calibrated using external calibration analysis (a series of standards of known Al and Zr concentrations were prepared and measured externally to the samples to produce a linear calibration) and measured by Mr P. Holdship (University of Oxford) on a Perkin Elmer Elan 6100DRC ICP-MS.

Scanning electron microscopy (SEM) analysis was performed on a JOEL JSM 6610LV scanning electron microscope with an accelerating voltage of 3.0 kV. Samples were spread on carbon tape adhered to an SEM stage. Before imaging, the polyethylene samples were coated with a thin platinum layer (10 nm thickness) to prevent charging and to improve image quality.

Scanning electron microscopy energy dispersive X-ray (SEM-EDX) spectroscopy was performed by Mrs Jennifer A. Holter (David Cockayne Centre for Electron Microscopy, Oxford Materials) on a Carl Zeiss Merlin high resolution field emission gun SEM at a voltage of 20 kV fitted with Zeiss A-STEM detector. EDX spectra were measured using an Oxford instruments Xmax 150. Samples of sMMAO were spread on silicon nitride membranes (200 μm substrate thickness), and quickly transferred from a vial sealed under N_2 to the instrument vacuum antechamber. SEM-EDX elemental mapping and line scan analysis were carried out using the AZtecLive software package.

Differential scanning calorimetry experiments were performed on a Mettler Toledo TGA/DSC 1 System in a temperature range of 25–180 °C at a rate of 10 °C min^{-1}.

Gel permeation chromatography (GPC) samples were collected by Ms Liv Thorbu at Norner AS (Norway) on a high temperature gel permeation chromatograph with a IR5 infrared detector (GPC-IR5). Samples were prepared by dissolution in 1,2,4-trichlorobenzene (TCB) containing 300 ppm of 3,5-di-*tert*-butyl-4-hydroxytoluene (BHT) at 160 °C for 90 minutes and then filtered with a 10 μm SS filter before being passed through the GPC column. The samples were run under a flow rate of 0.5 mL/min

using TCB containing 300 ppm of BHT as mobile phase with 1 mg/mL BHT added as a flow rate marker. The GPC column and detector temperature were set at 145 and 160 °C respectively.

1.3. Syntheses and characterisation data

General procedures for immobilisation of metallocene pre-catalysts

To a Schlenk flask charged with sMAO (60.6 mg_{Al}, 2.24 $mmol_{Al}$) and (EBI)$ZrCl_2$ (4.7 mg, 0.011 mmol) was added toluene (40 mL), and the resulting orange dispersion was heated at 80 °C for 1 h with regular swirling. The mixture was allowed to cool to room temperature and a pink-orange solid settled below a colourless supernatant solution. The supernatant was removed by filtration and the remaining slurry was dried *in vacuo* overnight, to afford a free-flowing orange solid.
Complete immobilisation of (EBI)$ZrCl_2$ on the support after heating/swirling was judged by a colourless toluene filtrate and confirmed for the control sMAO catalyst by ICP-MS: Al, 38.89 wt%; Zr, 0.67 wt%; mol_{Al}/mol_{Zr} = 196.

1.4. Ethylene polymerisation studies

The solid supported catalyst (10.0 mg), triisobutylaluminium scavenger (150 mg), and hexane (50 mL) were added to a high-pressure Rotaflo ampoule. Ethylene gas was continuously fed into the ampoule at 2 bar overpressure during polymerisation at 70 °C. After 30 minutes, the reaction was stopped by removing the ampoule from the oil bath, and degassing *in vacuo*. The polymer was isolated on a frit, washed with pentane (50 mL) and vacuum dried at room temperature for 1 h. Each polymerisation experiment was conducted at least twice to ensure the reproducibility of the corresponding outcome, and mean activities are quoted in units of $kg_{PE}mol_{Zr}^{-1}h^{-1}$.

2. Additional characterising data

2.1. Solution NMR spectroscopy

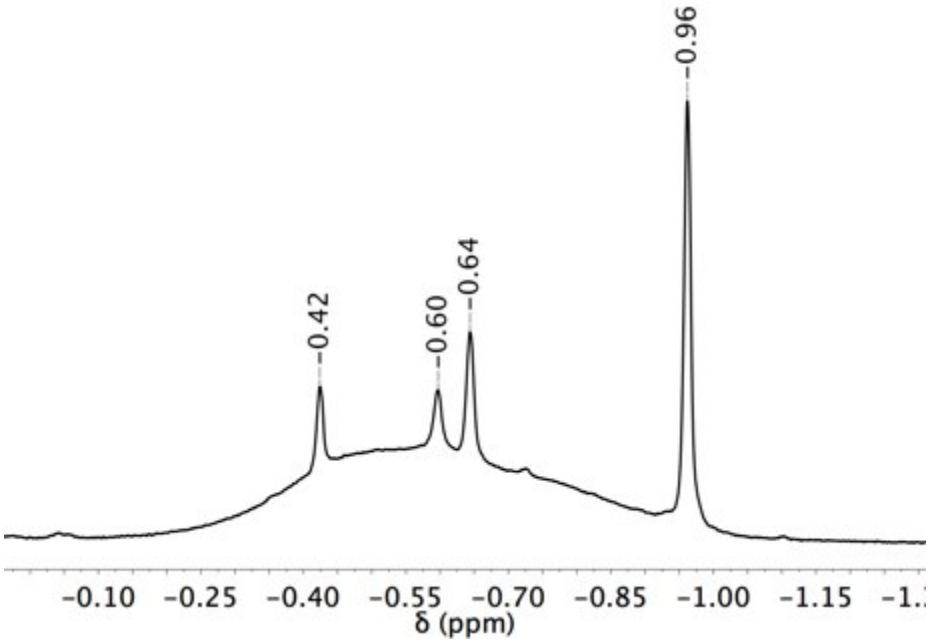

Figure S1 Selected region of the ^{1}H NMR spectrum of $Cp_2Zr(C_6F_5)_2$–sMAO ($[Al_{sMAO}]_0/[Zr]_0 = 50$) catalyst in THF-$d_8$.

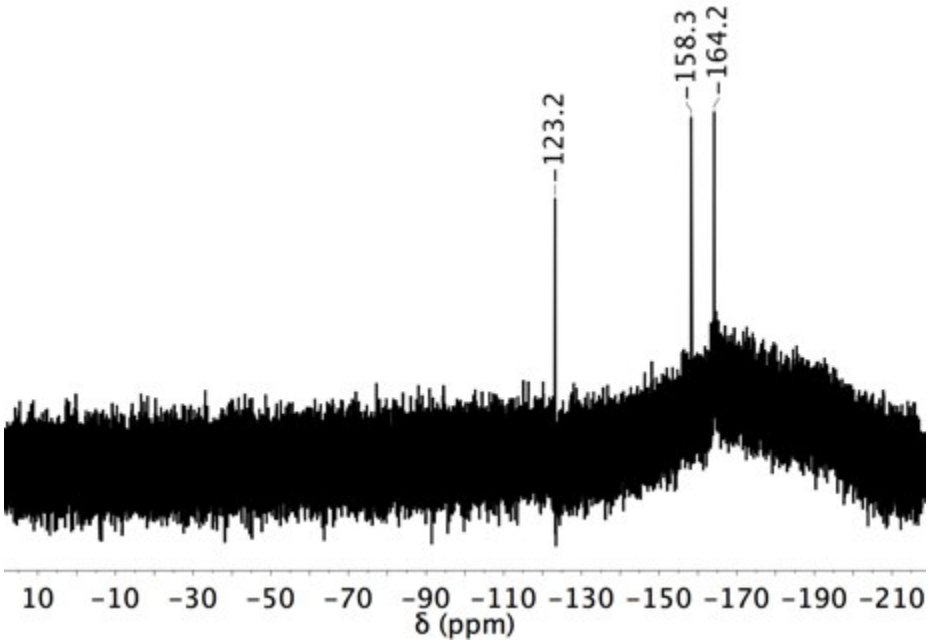

Figure S2 ^{19}F{^{1}H} NMR spectrum of $Cp_2Zr(C_6F_5)_2$–sMAO ($[Al_{sMAO}]_0/[Zr]_0 = 50$) catalyst in THF-$d_8$.

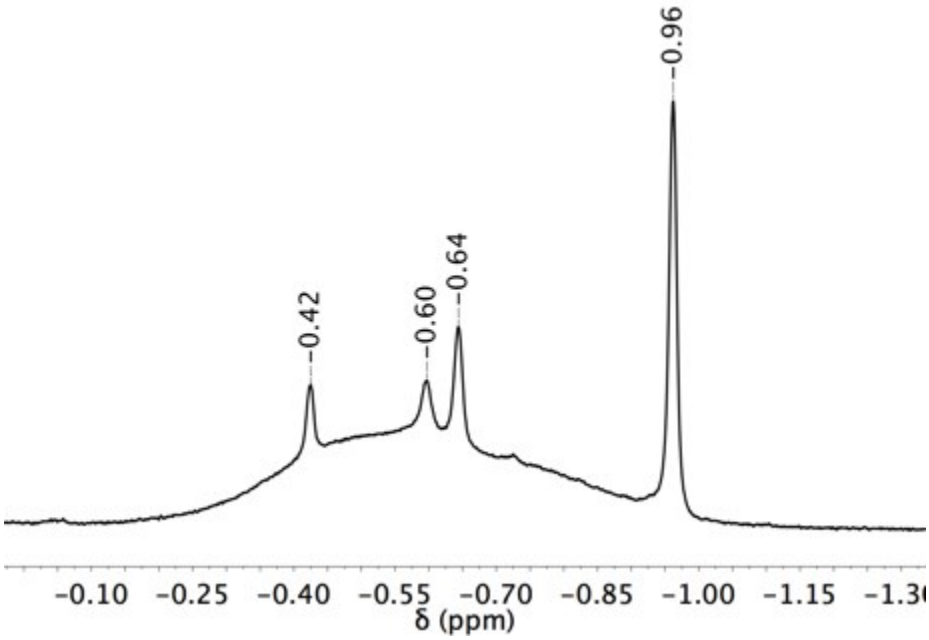

Figure S3 Selected region of the ^{1}H NMR spectrum of $Cp_2Zr(C_6F_5)_2$–sMAO ($[Al_{sMAO}]_0/[Zr]_0 = 50$) catalyst in THF-$d_8$.

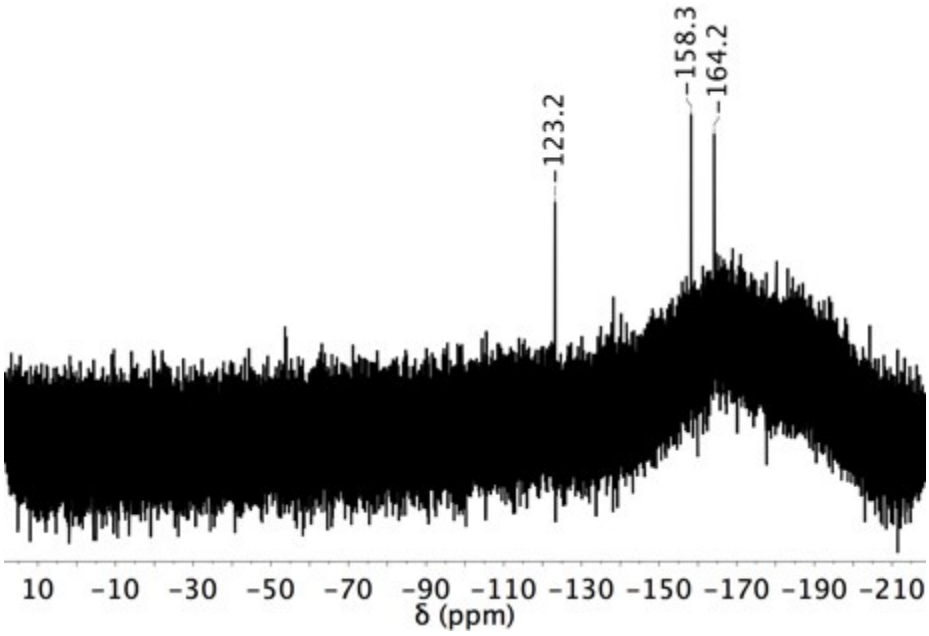

Figure S4 $^{19}F\{^{1}H\}$ NMR spectrum of $Cp_2Zr(C_6F_5)_2$–sMAO ($[Al_{sMAO}]_0/[Zr]_0 = 50$) catalyst in THF-$d_8$.

2.2. Solid state NMR spectroscopy

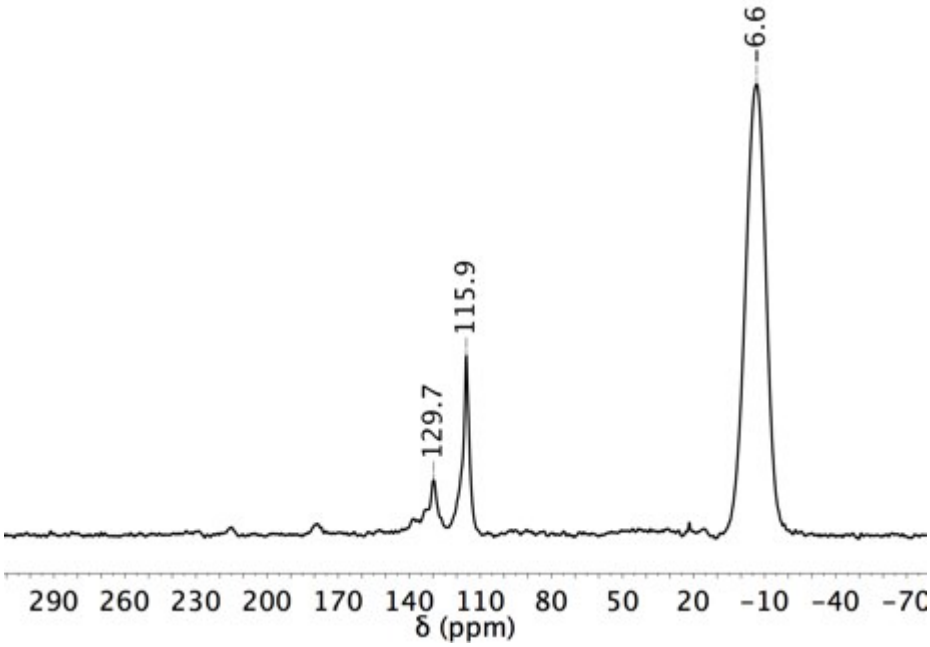

Figure S5 $^{1}H \rightarrow ^{13}C$ CP-MAS SSNMR spectrum (10 kHz spinning) of Cp_2ZrCl_2–sMAO ($[Al_{sMAO}]_0/[Zr]_0 = 25$) catalyst.

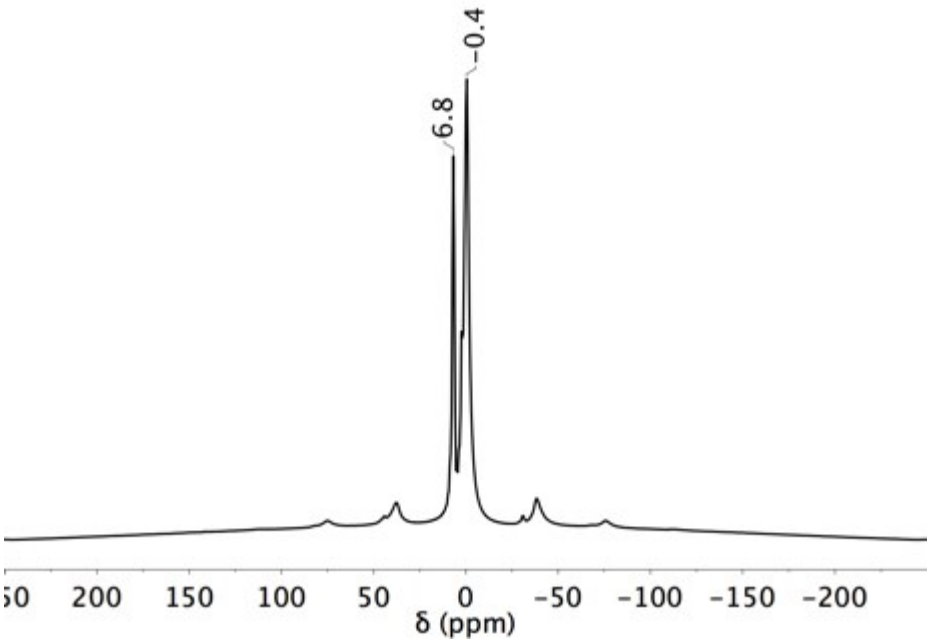

Figure S6 ^{1}H DEPTH SSNMR spectrum (15 kHz spinning) of Cp_2ZrCl_2–sMAO ($[Al_{sMAO}]_0/[Zr]_0 = 25$) catalyst.

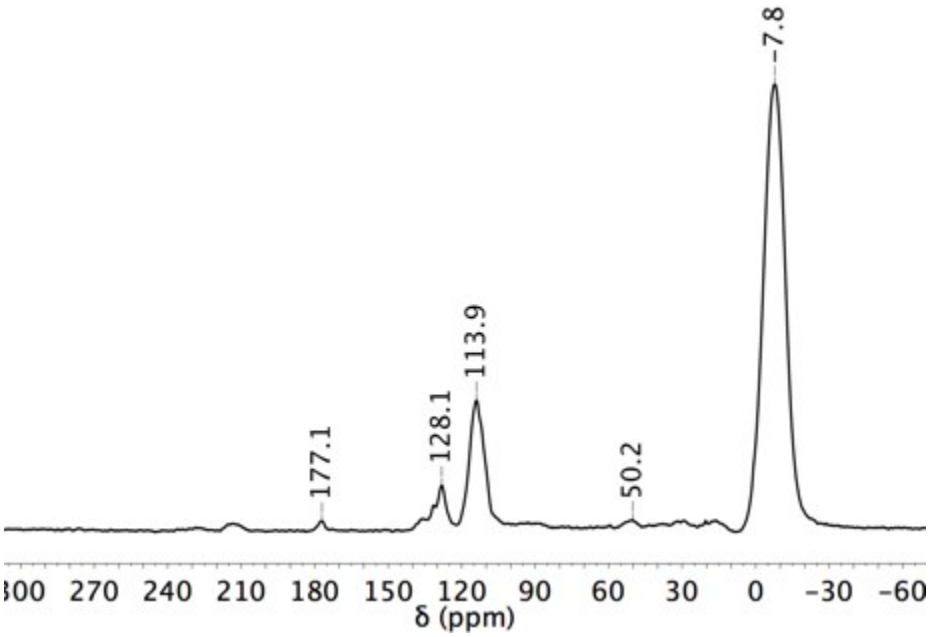

Figure S7 $^{1}H \rightarrow ^{13}C$ CP-MAS SSNMR spectrum (10 kHz spinning) of Cp_2ZrMe_2–sMAO ($[Al_{sMAO}]_0/[Zr]_0 = 25$) catalyst.

Figure S8 ^{1}H DEPTH SSNMR spectrum (15 kHz spinning) of Cp_2ZrMe_2–sMAO ($[Al_{sMAO}]_0/[Zr]_0 = 25$) catalyst.

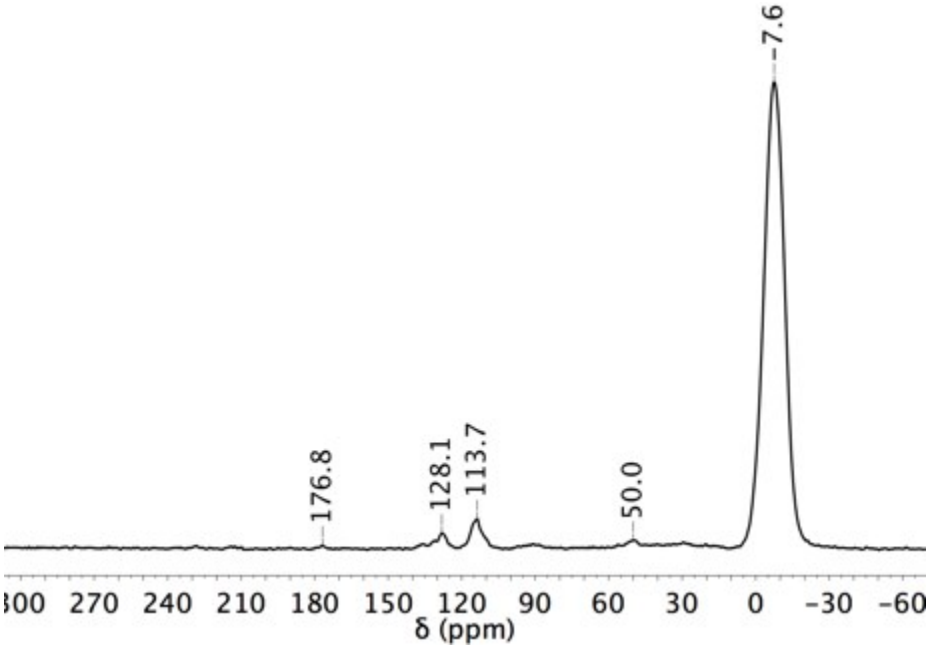

Figure S9 $^{1}H \rightarrow ^{13}C$ CP-MAS SSNMR spectrum (10 kHz spinning) of $Cp_2Zr(^{13}CH_3)_2$–sMAO ($[Al_{sMAO}]_0/[Zr]_0 = 50$) catalyst.

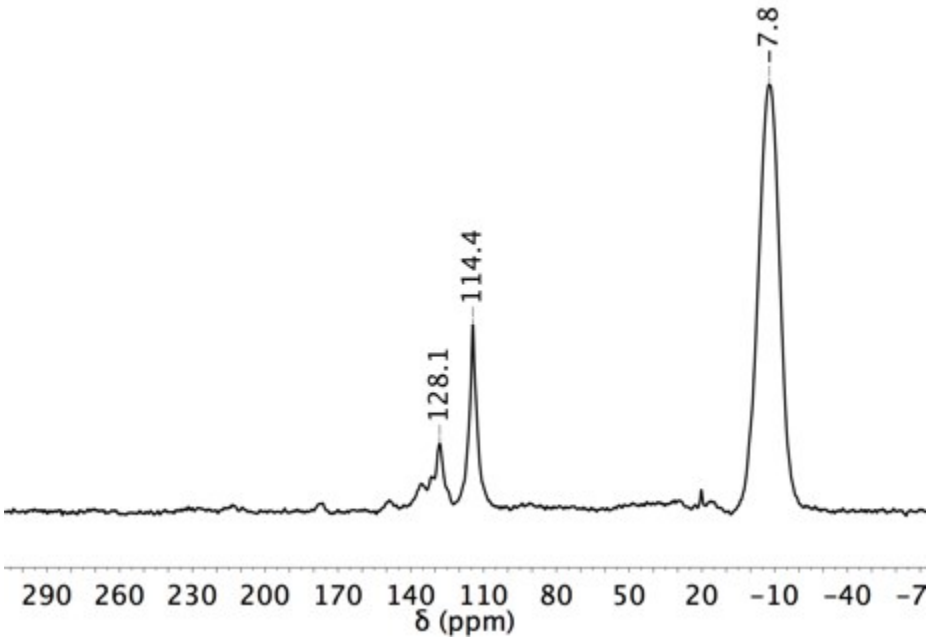

Figure S10 $^{1}H \rightarrow ^{13}C$-{^{1}H,^{19}F} CP-MAS SSNMR spectrum (10 kHz spinning) of $Cp_2Zr(C_6F_5)_2$–sMAO ($[Al_{sMAO}]_0/[Zr]_0 = 25$) catalyst.

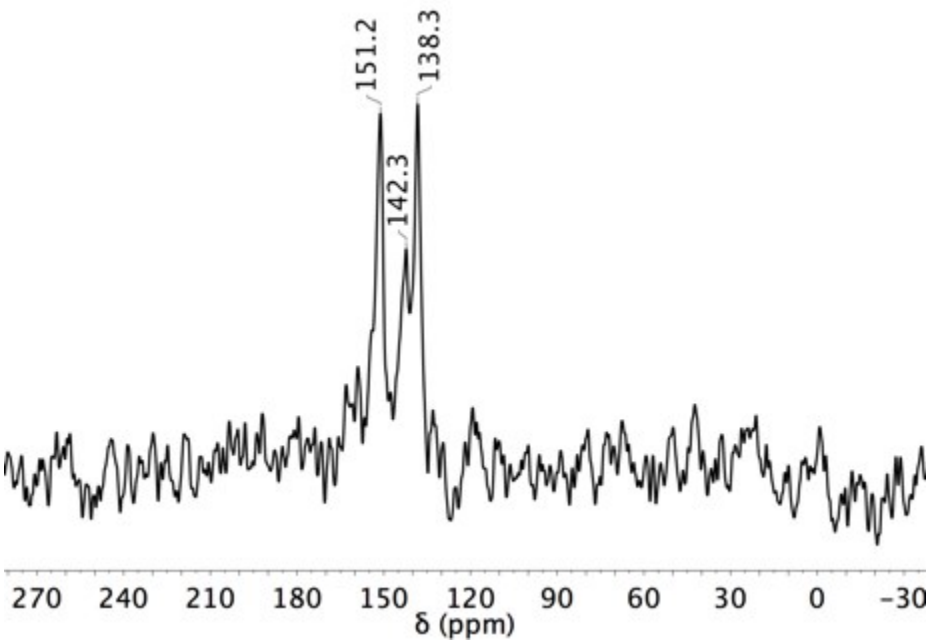

Figure S11 $^{19}F \rightarrow {}^{13}C$-{$^{1}H$,$^{19}F$} CP-MAS SSNMR spectrum (10 kHz spinning) of $Cp_2Zr(C_6F_5)_2$–sMAO ($[Al_{sMAO}]_0/[Zr]_0 = 25$) catalyst.

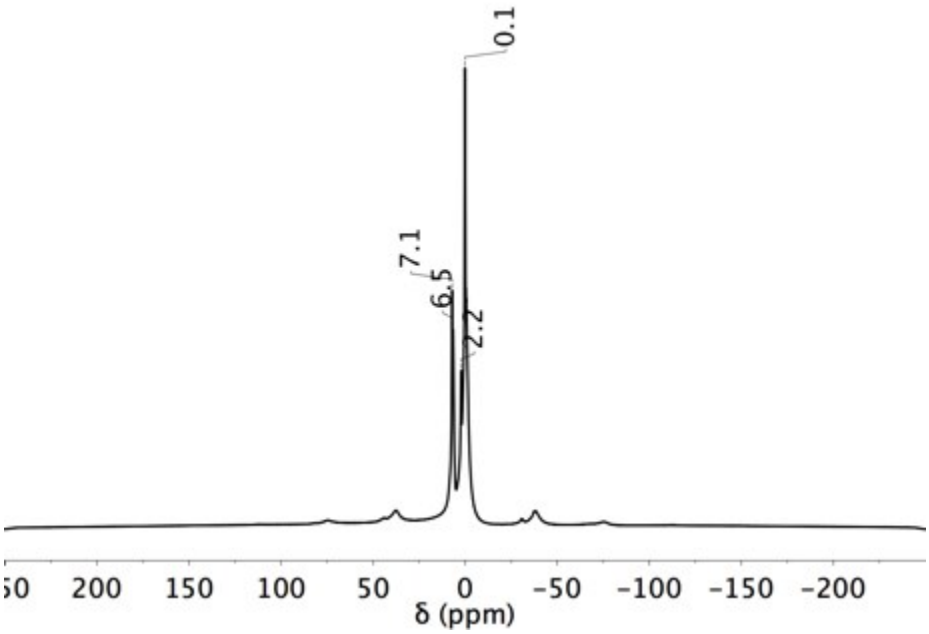

Figure S12 ^{1}H DEPTH SSNMR spectrum (15 kHz spinning) of $Cp_2Zr(C_6F_5)_2$–sMAO ($[Al_{sMAO}]_0/[Zr]_0 = 25$) catalyst.

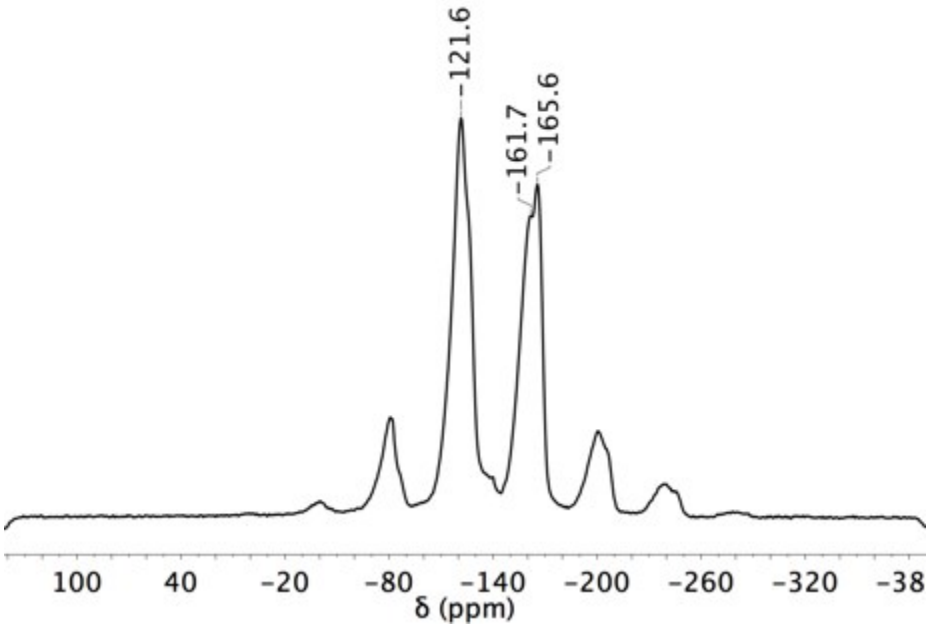

Figure S13 ^{19}F DEPTH SSNMR spectrum (10 kHz spinning) of $Cp_2Zr(C_6F_5)_2$–sMAO ($[Al_{sMAO}]_0/[Zr]_0 = 25$) catalyst.

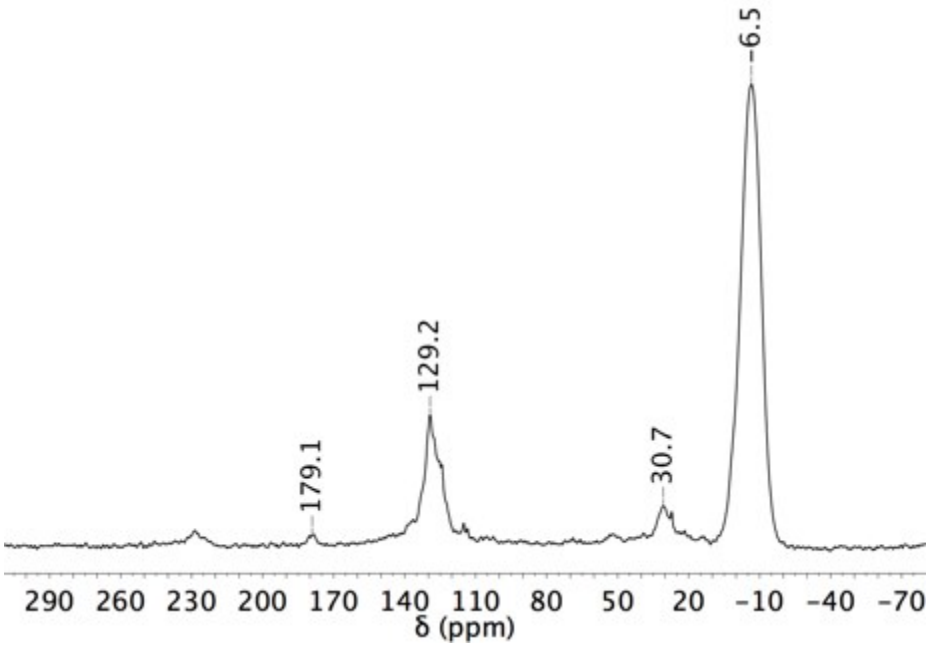

Figure S14 $^{1}H \rightarrow {}^{13}C$ CP-MAS SSNMR spectrum (10 kHz spinning) of (EBI)$ZrCl_2$–sMAO ($[Al_{sMAO}]_0/[Zr]_0 = 50$) catalyst.

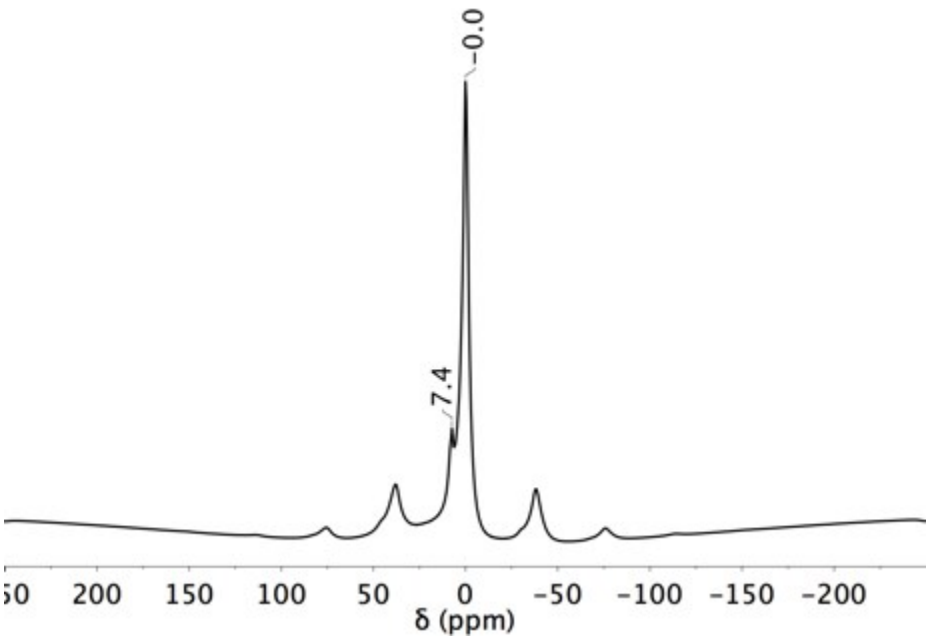

Figure S15 ^{1}H DEPTH SSNMR spectrum (15 kHz spinning) of (EBI)$ZrCl_2$–sMAO ($[Al_{sMAO}]_0/[Zr]_0 = 50$) catalyst.

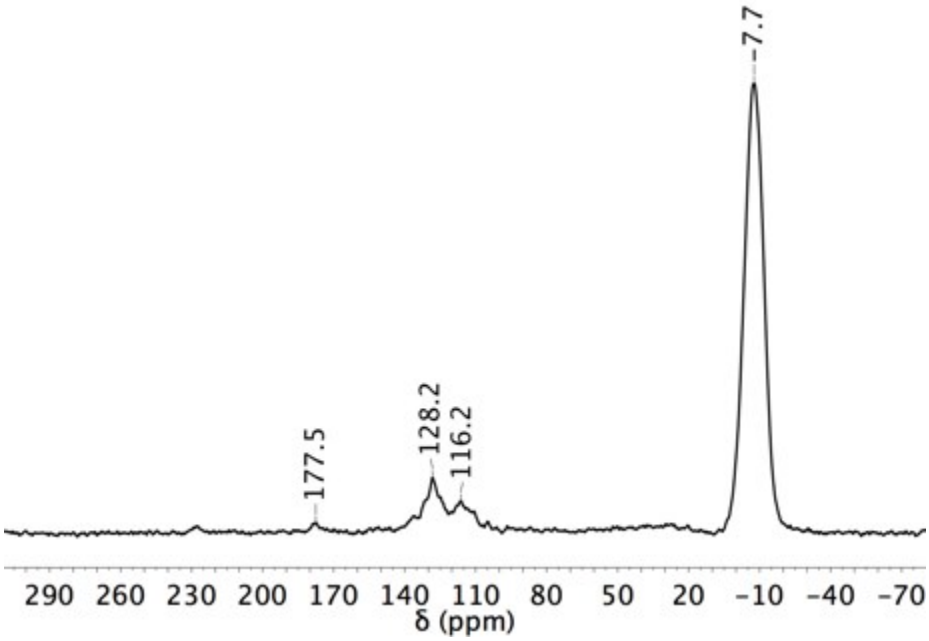

Figure S16 $^{1}H \rightarrow {}^{13}C$ CP-MAS SSNMR spectrum (10 kHz spinning) of $Me_2Si(C_5H_4)_2ZrCl_2$–sMAO ($[Al_{sMAO}]_0/[Zr]_0 = 50$) catalyst.

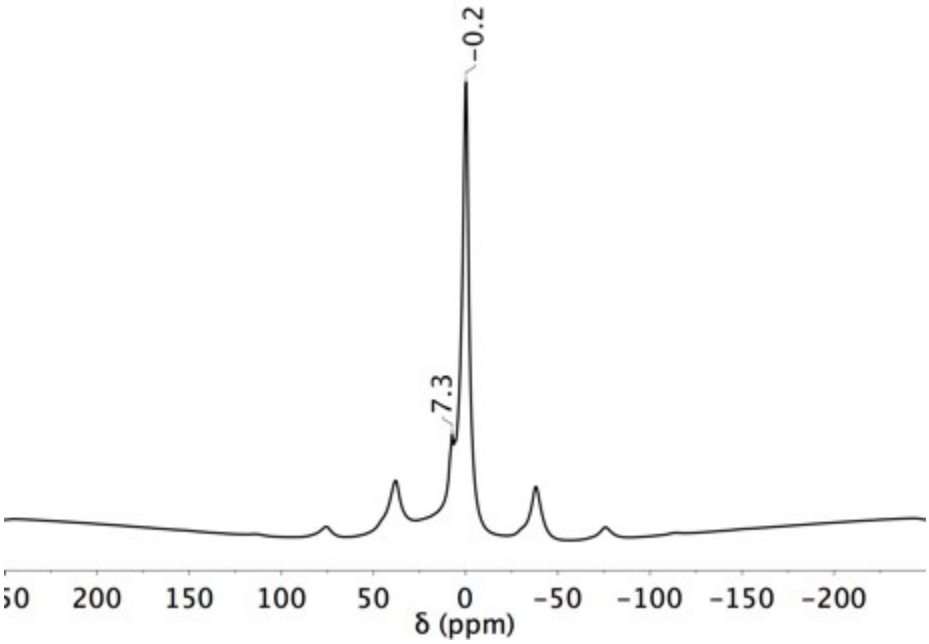

Figure S17 ^{1}H DEPTH SSNMR spectrum (15 kHz spinning) of $Me_2Si(C_5H_4)_2ZrCl_2$–sMAO ($[Al_{sMAO}]_0/[Zr]_0 = 50$) catalyst.

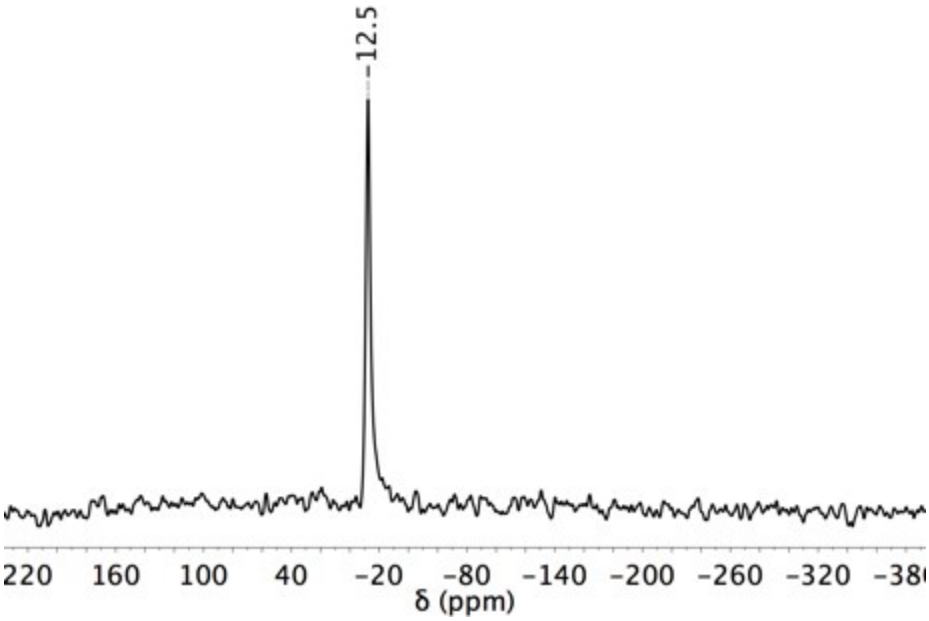

Figure S18 $^{1}H \rightarrow {}^{29}Si$ CP-MAS SSNMR spectrum (10 kHz spinning) of $Me_2Si(C_5H_4)_2ZrCl_2$–sMAO ($[Al_{sMAO}]_0/[Zr]_0 = 50$) catalyst.

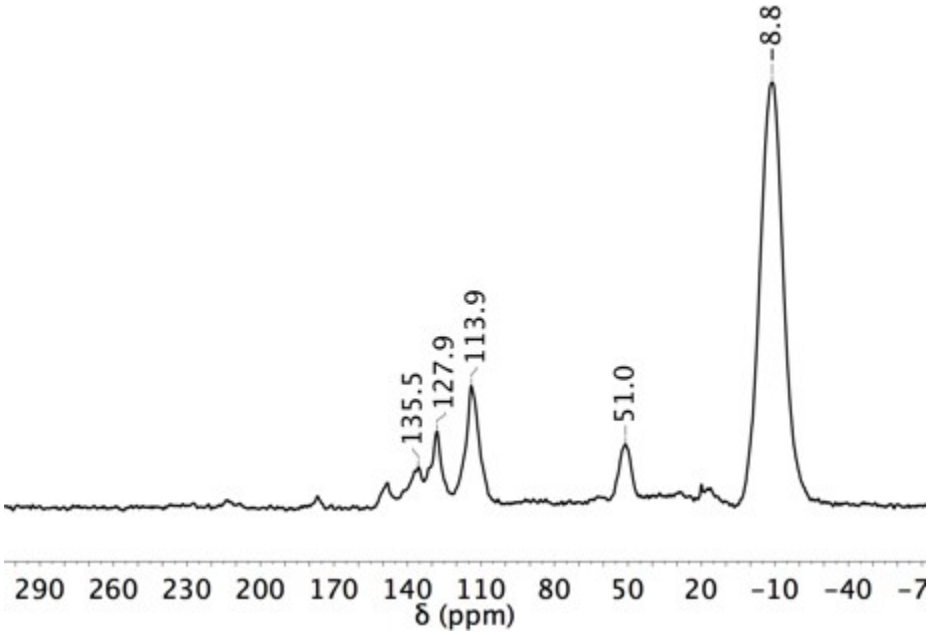

Figure S19 $^{1}H \rightarrow ^{13}C$-{^{1}H,^{19}F} CP-MAS SSNMR spectrum (10 kHz spinning) of Cp_2ZrMe_2–sMAO(C_6F_5) ($[Al_{sMAO}]_0/[Zr]_0 = 25$) catalyst.

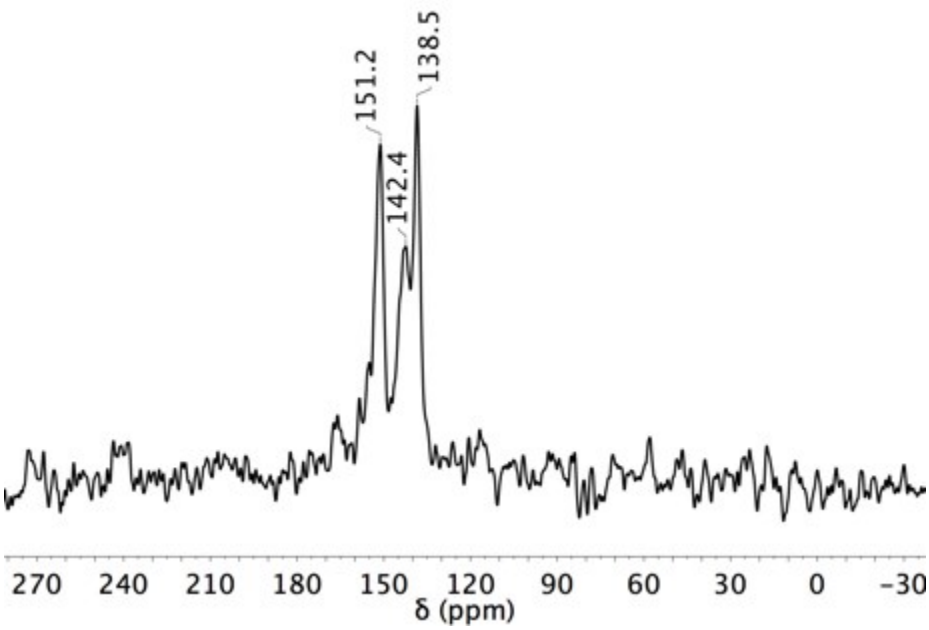

Figure S20 $^{19}F \rightarrow ^{13}C$-{$^{1}H$,$^{19}F$} CP-MAS SSNMR spectrum (10 kHz spinning) of Cp_2ZrMe_2–sMAO(C_6F_5) ($[Al_{sMAO}]_0/[Zr]_0 = 25$) catalyst.

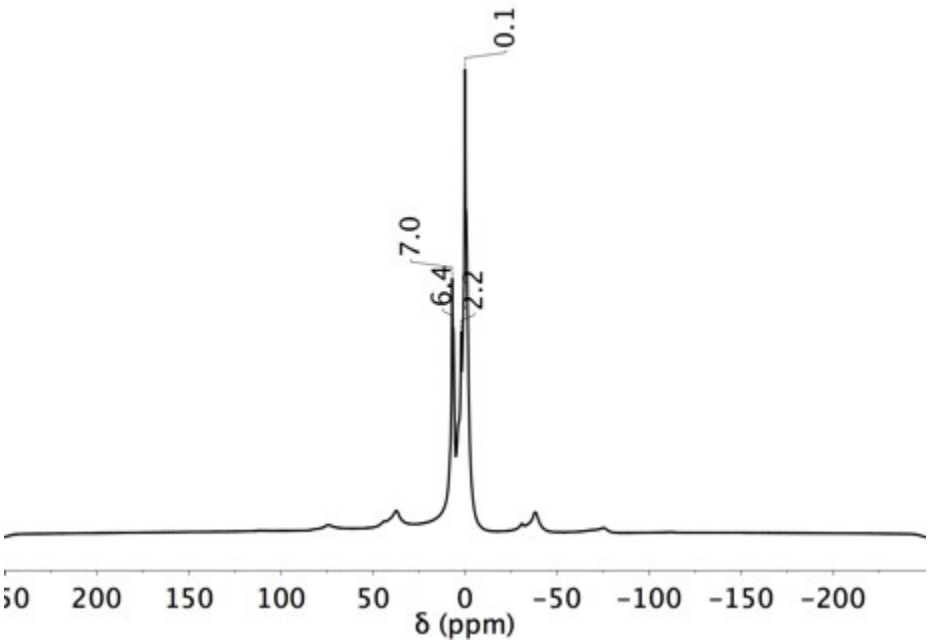

Figure S21 ^{1}H DEPTH SSNMR spectrum (15 kHz spinning) of Cp_2ZrMe_2–sMAO(C_6F_5) ($[Al_{sMAO}]_0/[Zr]_0 = 25$) catalyst.

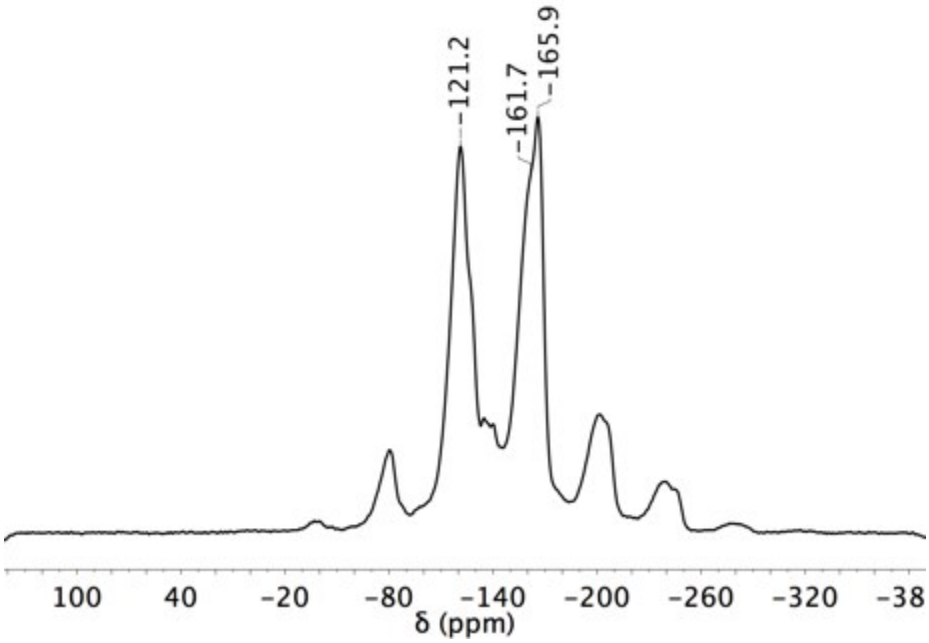

Figure S22 ^{19}F DEPTH SSNMR spectrum (10 kHz spinning) of Cp_2ZrMe_2–sMAO(C_6F_5) ($[Al_{sMAO}]_0/[Zr]_0 = 25$) catalyst.

2.3. Diffuse reflectance infrared Fourier transform (DRIFT) spectroscopy

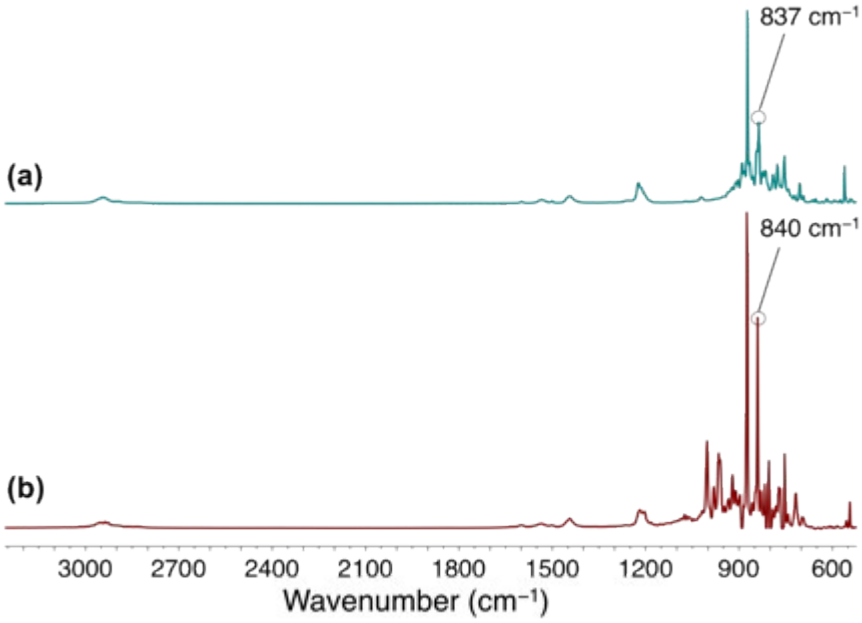

Figure S23 Normalised DRIFT spectra of (a) Cp_2ZrCl_2–sMAO and (b) Cp_2ZrMe_2–sMAO ($[Al_{sMAO}]_0/[Zr]_0 = 25$). Spectra are offset for clarity with IR bands assigned to Zr–Me species highlighted.

2.4. Scanning Electron Microscopy with Energy Dispersive X-ray (SEM-EDX) spectroscopy

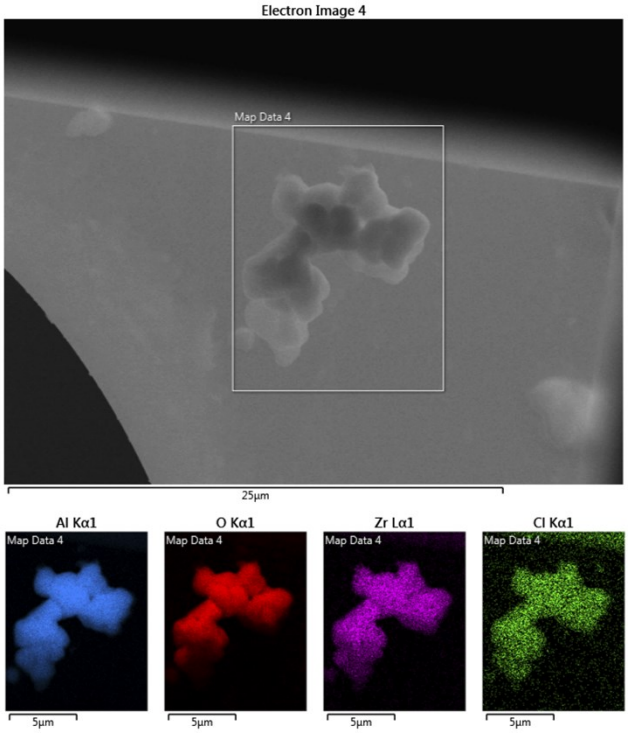

Figure S24 SEM micrograph of sMAO–$CpZrCl_2$ ($[Al_{sMAO}]_0/[Zr]_0 = 25$) particles with corresponding Al, (blue), O (red), Zr (purple) and Cl (green) elemental maps, as determined by EDX spectroscopy.

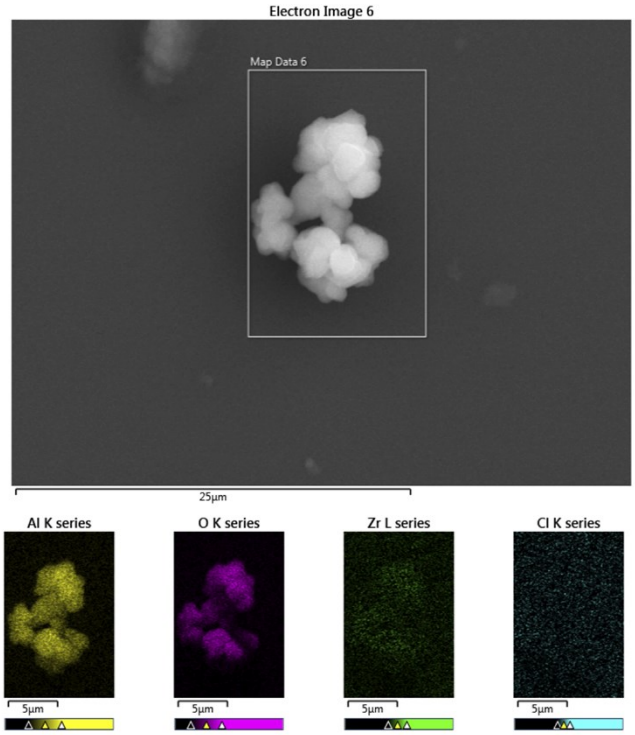

Figure S25 SEM micrograph of sMAO–$CpZrMe_2$ ($[Al_{sMAO}]_0/[Zr]_0 = 25$) particles with corresponding Al (yellow), O (purple), Zr (green) and Cl (sky blue) elemental maps, as determined by EDX spectroscopy.

2.5. Scanning electron microscopy (SEM) imaging

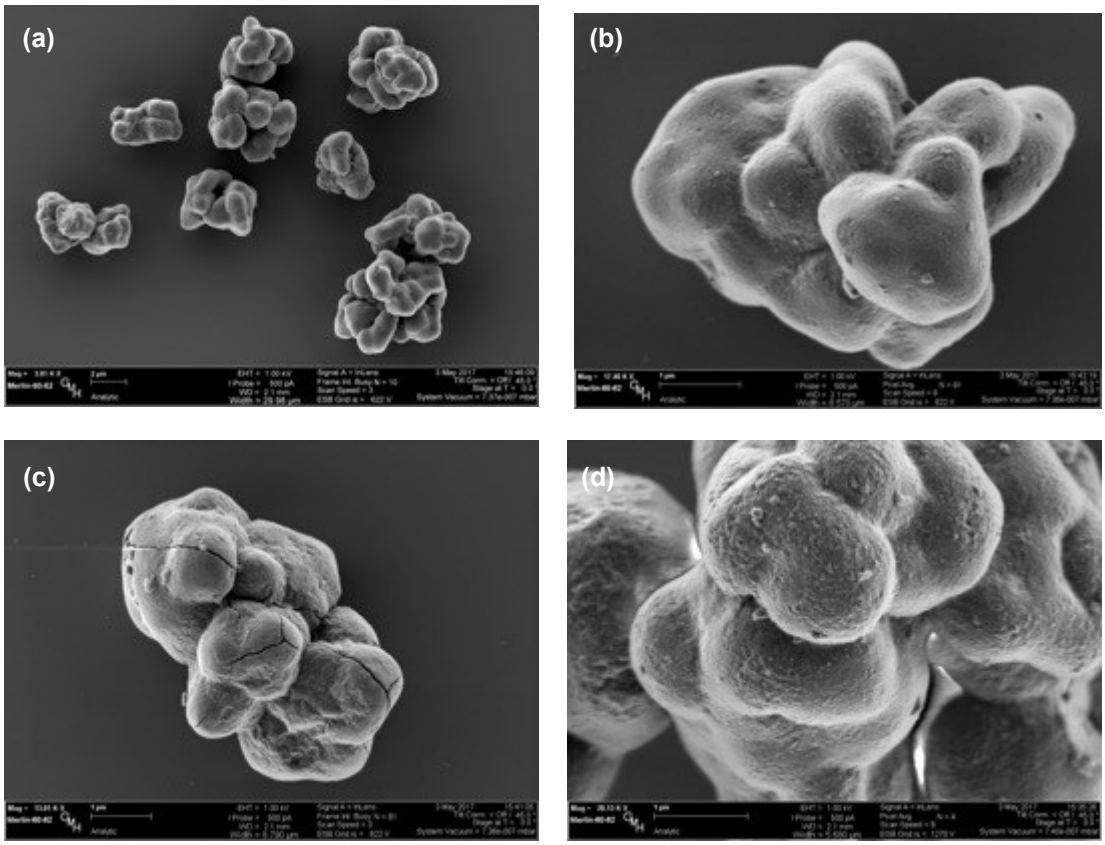

Figure S26 SEM images at (a)×3.81k, (b)×17.4k, (c)×13.0k and (d)×63.6k magnification of a sample of Cp_2ZrCl_2–sMAO ($[Al_{sMAO}]_0/[Zr]_0 = 50$) catalyst.

3. Slurry phase ethylene polymerisation studies

3.1. Additional polymerisation data

Table S1 Laboratory scale ethylene polymerisation for supported complex–sMAO catalysts at target loading $[Al_{sMAO}]_0/[Zr]_0 = 50$.

Complex	Activity ($kg_{PE}mol_{Zr}^{-1}h^{-1}$)	SD	Productivity ($kg_{PE}g_{cat}^{-1}h^{-1}$)	SD
Cp_2ZrCl_2	953.8	16.9	0.2629	0.0047
Cp_2ZrMe_2	1049.1	24.0	0.2908	0.0067
Cp_2ZrBr_2	516.6	141.6	0.1380	0.0378
$Cp_2Zr(C_6H_5)_2$	977.3	6.4	0.2648	0.0017
$Cp_2Zr(C_6F_5)_2$	1164.4	116.0	0.2955	0.0294
$Cp_2Zr(OC_6F_5)_2$	910.5	81.0	0.2328	0.0207
$^{n\mathrm{Bu}}Cp_2ZrCl_2$	1929.9	147.3	0.5097	0.0389
$(EBI)ZrCl_2$	3643.8	61.0	0.9713	0.0163
$Me_2Si(C_5H_4)_2ZrCl_2$	292.3	0.4	0.0787	0.0001
$Me_2Si(C_5H_4)_2ZrMe_2$	534.3	14.0	0.1455	0.0038

Immobilisation conditions: 80 °C, 1 h, toluene. Polymerisation conditions: 10 mg catalyst, 2 bar C_2H_4, 70 °C, 30 minutes, $[Al_{TIBA}]_0/[Zr]_0 = 1000$, hexane (50 mL).

Table S2 Laboratory scale ethylene polymerisation for supported catalysts at target loading $[Al_{sMAO}]_0/[Zr]_0 = 25$.

Complex	Solid support	Activity ($kg_{PE}mol_{Zr}^{-1}h^{-1}$)	SD	Productivity ($kg_{PE}g_{cat}^{-1}h^{-1}$)	SD
Cp_2ZrMe_2	sMAO	560.4	26.1	0.2887	0.0067
Cp_2ZrMe_2	sMMAO(C_6F_5)	772.0	85.8	0.3442	0.0382
$Cp_2Zr(C_6F_5)_2$	sMAO	775.7	4.5	0.2703	0.0016

Immobilisation conditions: 80 °C, 1 h, toluene. Polymerisation conditions: 10 mg catalyst, 2 bar C_2H_4, 70 °C, 30 minutes, $[Al_{TIBA}]_0/[Zr]_0 = 1000$, hexane (50 mL).

Table S3 Laboratory scale ethylene polymerisation data for supported complex–sMAO catalysts with various $[Al_{sMAO}]_0/[Zr]_0$ target loadings.

Precursor	$[Al_{sMAO}]_0/[Zr]_0$ loading	Activity ($kg_{PE}mol_{Zr}^{-1}h^{-1}$)	SD	Productivity ($kg_{PE}g_{Cat}^{-1}h^{-1}$)	SD
None	0	0		0	
Cp_2ZrCl_2	25	453	1	0.228	0.0003
	50	954	24	0.263	0.007
	100	2440	50	0.347	0.007
	200	3664	277	0.266	0.020
	300	4939	47	0.241	0.0030
Cp_2ZrMe_2	25	560	37	0.289	0.019
	50	1081	19	0.299	0.005
	100	2208	15	0.314	0.0022
	200	3682	16	0.268	0.0011
	300	4624	19	0.262	0.0011

Immobilisation conditions: 80 °C, 1 h, toluene. Polymerisation conditions: 10 mg catalyst, 2 bar C_2H_4, 70 °C, 30 minutes, $[Al_{TIBA}]_0/[Zr]_0$ = 1000, hexane (50 mL).

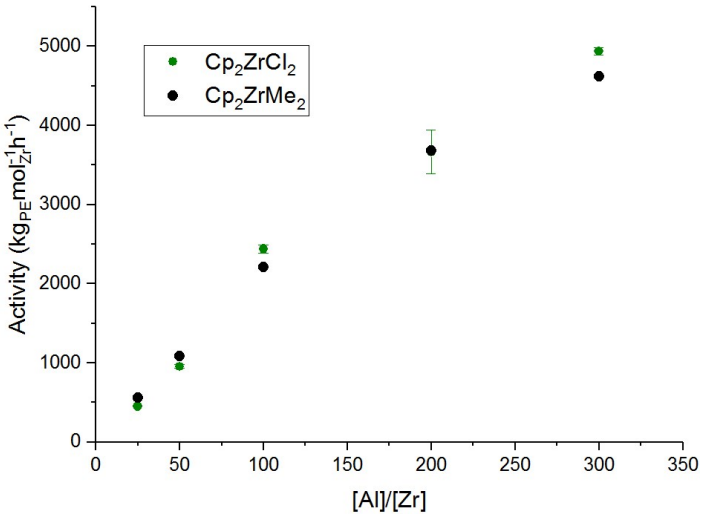

Figure S27 Ethylene polymerisation activities for sMAO–Cp_2ZrCl_2 (green) and sMAO–Cp_2ZrMe_2 (black) at variable $[Al_{sMAO}]_0/[Zr]_0$ target loadings.

3.2. Differential scanning calorimetry (DSC) of polyethylene samples

Table S4 Polyethylene temperature of melting (T_m) and crystallisation (T_c), enthalpy of melting and crystallisation produced using using sMAO–complex catalysts at $[Al_{sMAO}]_0/[Zr]_0 = 50$.

Complex	T_m (° C)	T_c (° C)	ΔH_m (J g^{-1})	ΔH_c (J g^{-1})
Cp_2ZrBr_2	135	117	140	143
$Cp_2Zr(C_6F_5)_2$	135	117	154	154
$Cp_2Zr(OC_6F_5)_2$	135	116	160	170
$Me_2Si(C_5H_4)_2ZrCl_2$	129	118	165	168

Polymerisation conditions: 10 mg catalyst, 2 bar C_2H_4, 70 °C, 30 minutes, $[Al_{TIBA}]_0/[Zr]_0 = 1000$, hexane (50 mL).

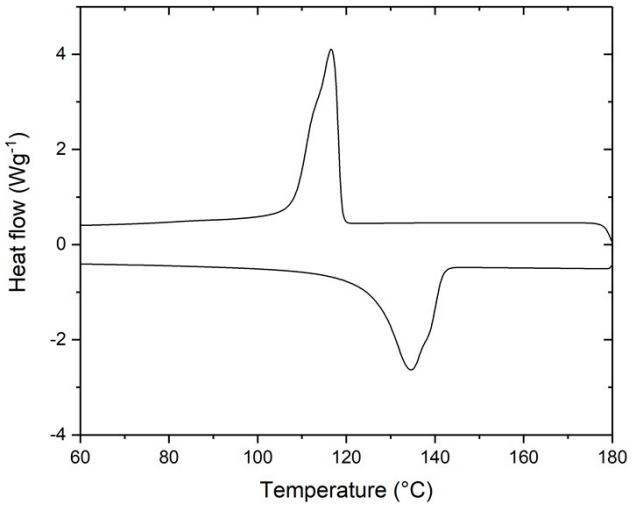

Figure S28 DSC plot showing the first cooling cycle and second heating cycle for the polyethylene sample (4.5 mg) produced using sMAO-supported Cp_2ZrBr_2.

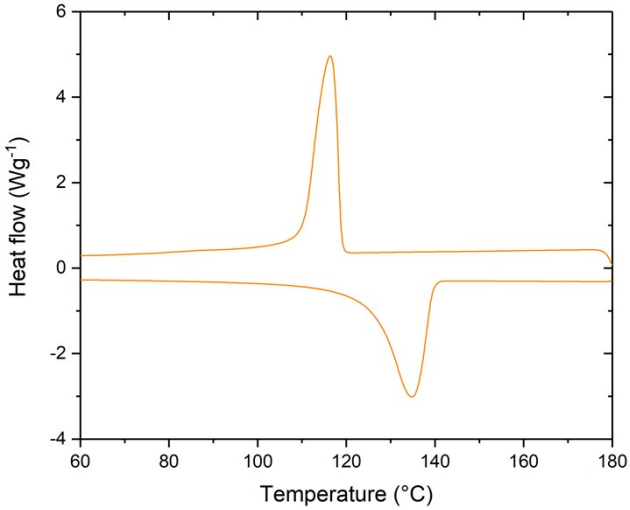

Figure S29 DSC plot showing the first cooling cycle and second heating cycle for a polyethylene sample (3.6 mg) produced using sMAO-supported $Cp_2Zr(C_6F_5)_2$.

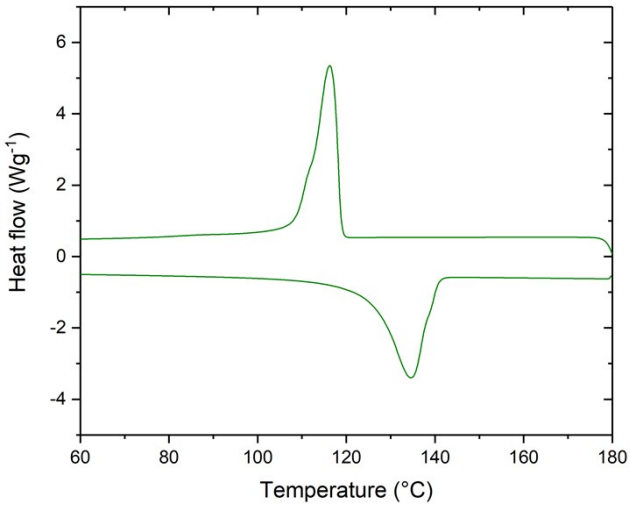

Figure S30 DSC plot showing the first cooling cycle and second heating cycle for a polyethylene sample (3.2 mg) produced using sMAO-supported $Cp_2Zr(OC_6F_5)_2$.

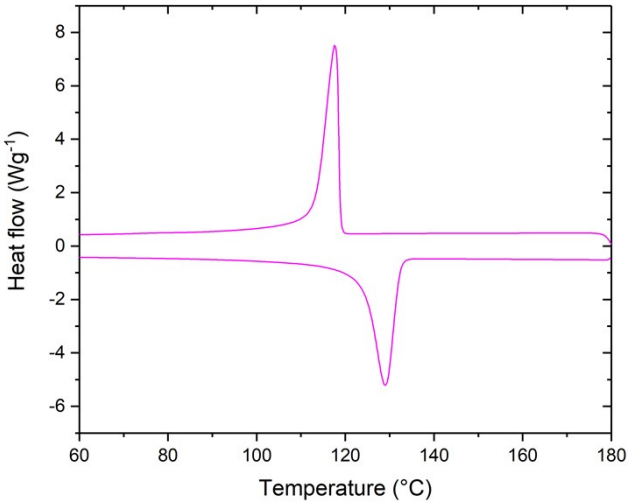

Figure S31 DSC plot showing the first cooling cycle and second heating cycle for a polyethylene sample (3.7 mg) produced using sMAO-supported $Me_2Si(C_5H_4)_2ZrCl_2$.

3.3. Scanning electron microscopy (SEM) imaging of polyethylene samples

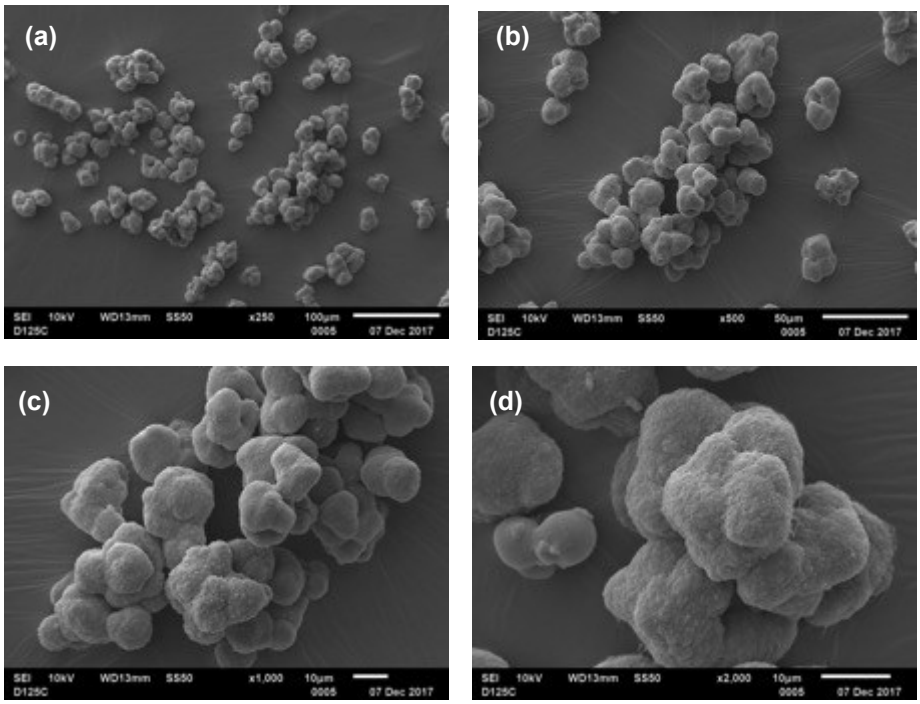

Figure S32 SEM images at (a)×250, (b)×500, (c)×1000 and (d)×2000 magnification of PE samples produced from a Cp_2ZrCl_2–sMAO catalyst system.

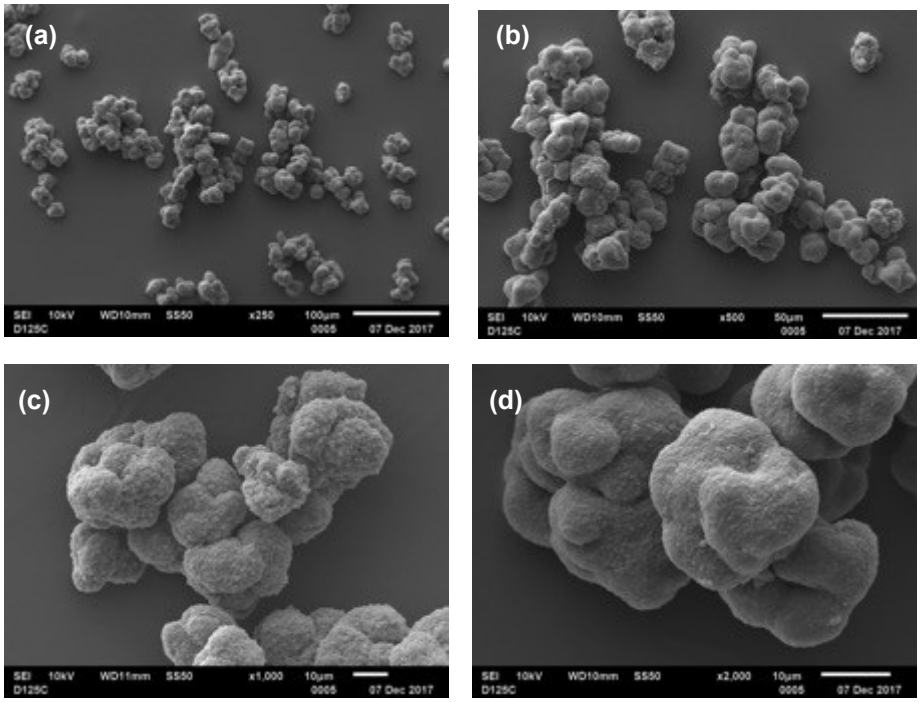

Figure S33 SEM images at (a)×250, (b)×500, (c)×1000 and (d)×2000 magnification of PE samples produced from a Cp_2ZrMe_2–sMAO catalyst system.

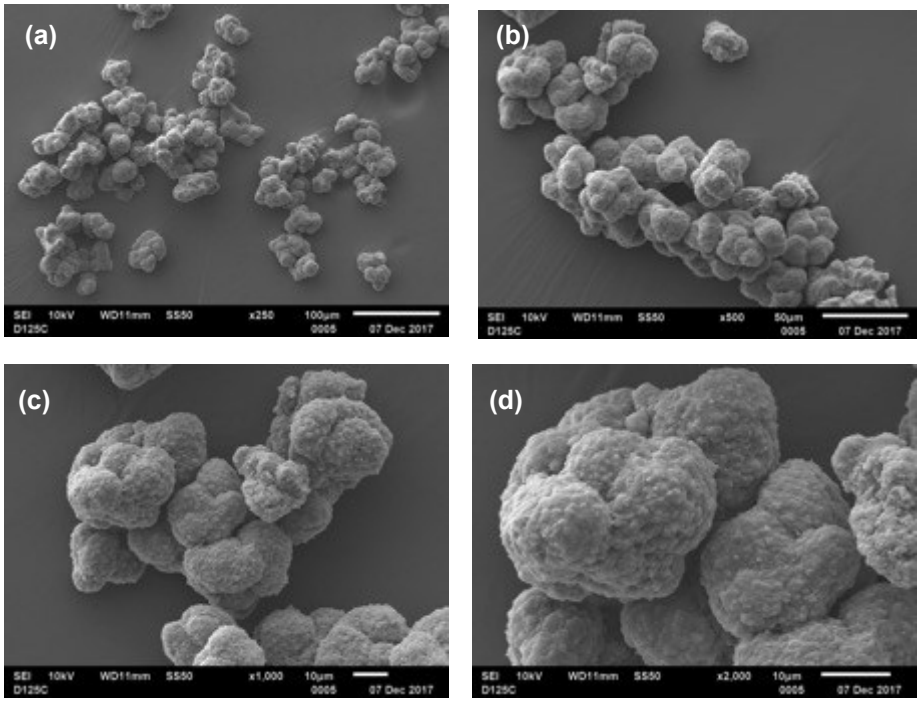

Figure S34 SEM images at (a)×250, (b)×500, (c)×1000 and (d)×2000 magnification of PE samples produced from a $^{n\mathrm{Bu}}Cp_2ZrCl_2$–sMAO catalyst system.

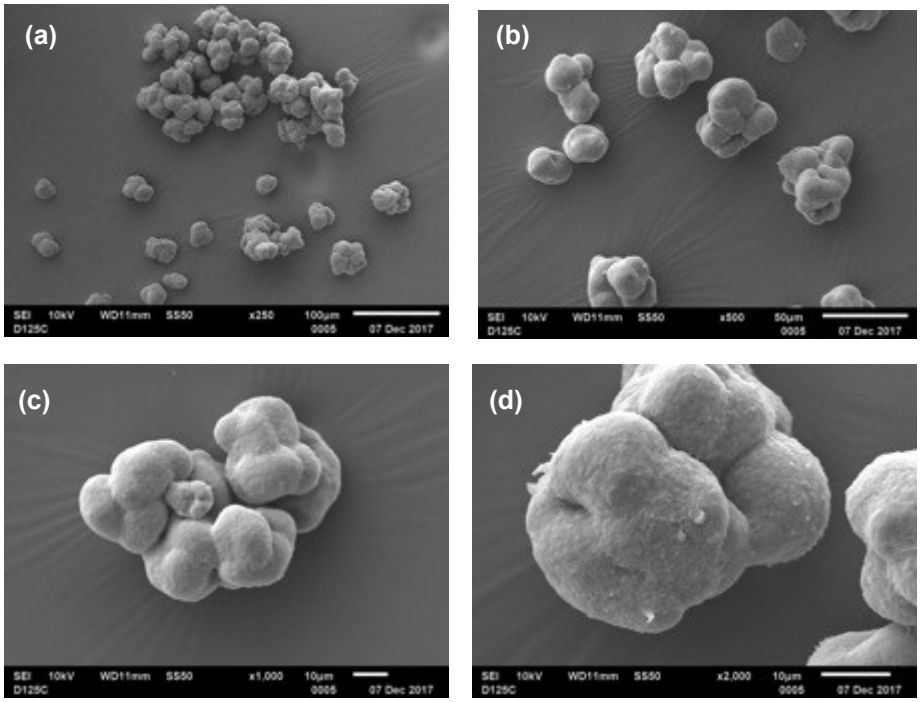

Figure S35 SEM images at (a)×250, (b)×500, (c)×1000 and (d)×2000 magnification of PE samples produced from a (EBI)$ZrCl_2$–sMAO catalyst system.

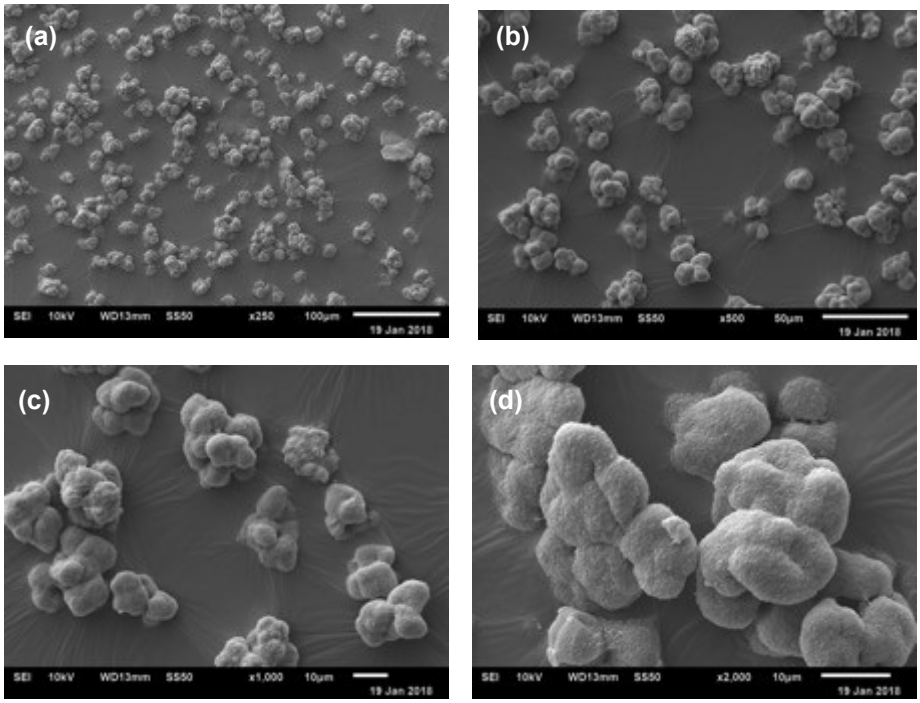

Figure S36 SEM images at (a)×250, (b)×500, (c)×1000 and (d)×2000 magnification of PE samples produced from a $Me_2Si(C_5H_4)_2ZrCl_2$–sMAO catalyst system.

3.4. Gel permeation chromatography (GPC) of polyethylene samples

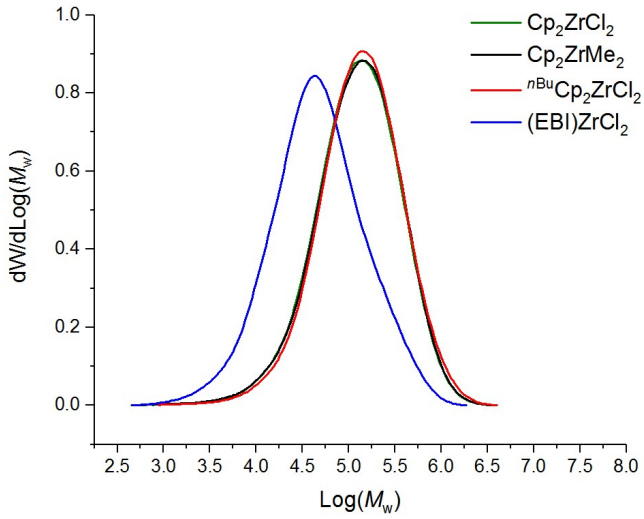

Figure S37 Overlaid GPC traces of PE samples produced from supported complex–sMAO catalysts at target loading $[Al_{sMAO}]_0/[Zr]_0 = 50$.

4. References

1 D. F. Shriver, *The Manipulation of Air-Sensitive Compounds*, Wiley-Interscience, 2nd edn. 1986.

2 A. B. Pangborn, M. A. Giardello, R. H. Grubbs, R. K. Rosen and F. J. Timmers, *Organometallics*, 1996, **15**, 1518–1520.

3 US Pat. 8,404,880 B2, 8,404,880 B2, 2013.

4 A. F. R. Kilpatrick, J.-C. Buffet, P. Nørby, N. H. Rees, N. P. Funnell, S. Sripothongnak and D. O'Hare, *Chem. Mater.*, 2016, **28**, 7444–7450.

5 Mestrelab Research SL Santiago de Compostela, Spain, 2008.

6 I. Hung and R. W. Schurko, *J. Phys. Chem. B*, 2004, **108**, 9060–9069.

7 F. H. Larsen, H. J. Jakobsen, P. D. Ellis and N. C. Nielsen, *J. Magn. Reson.*, 1998, **131**, 144–147.

8 M. Newville, *J Synchrotron Radiat*, 2001, **8**, 322–324.

9 B. Ravel and M. Newville, *J Synchrotron Radiat*, 2005, **12**, 537–541.

10 L. M. Kustov, *Top. Catal.*, 1997, **4**, 131–144.